minerals

MDPI

Article

Assessment of Potentially Toxic Elements in Technosols by Tailings Derived from Pb–Zn–Ag Mining Activities at San Quintín (Ciudad Real, Spain): Some Insights into the Importance of Integral Studies to Evaluate Metal Contamination Pollution Hazards

Mari Luz García-Lorenzo [1,*], Elena Crespo-Feo [1], Jose María Esbrí [2], Pablo Higueras [2], Patricia Grau [1], Isabel Crespo [1] and Ramón Sánchez-Donoso [3]

[1] Facultad de Ciencias Geológicas, Departamento de Mineralogía y Petrología, Universidad Complutense de Madrid, 28040 Madrid, Spain; ecrespo@ucm.es (E.C.-F.); patgrau@ucm.es (P.G.); isacresp@ucm.es (I.C.)
[2] Instituto de Geología Aplicada, Universidad de Castilla-La Mancha, Plaza Manuel Meca, 1, 13400 Almadén, Spain; josemaria.esbri@uclm.es (J.M.E.); pablo.higueras@uclm.es (P.H.)
[3] Facultad de Ciencias Geológicas, Departamento de Geodinámica, Estratigrafía y Paleontología, Universidad Complutense de Madrid, 28040 Madrid, Spain; ramons02@ucm.es
* Correspondence: mglorenzo@ucm.es; Tel.: +34-91-3945014

Received: 15 April 2019; Accepted: 31 May 2019; Published: 5 June 2019

Abstract: This work presents an integral methodological approach to assess the environmental potential hazards posed by metals and metalloids hosted by spolic technosols derived from old tailings from a mining operation for galena (PbS, with high Ag contents)-sphalerite (ZnS, with a varied cohort of trace elements contents) in central Spain. We studied the total and soluble concentrations and spatial distribution of Pb, Zn, Cd, As, and Fe and the mineralogy of these soils, as well as an ecotoxicological evaluation by means of bioassays. The indices assessing soil contamination such as pollution load index (*PI*) and natural mobility index (*NMI*) have been calculated. Furthermore, the phytotoxic effect of the soil samples has been determined and a chronic sediment toxicity test using the benthic ostracod *Heterocypris incongruens* was applied. The geochemical study of 33 spolic technosols samples indicates large to extremely large metal and metalloid total contents: up to 48,600 mg kg^{-1} Pb, 34,000 mg kg^{-1} Zn, 500 mg kg^{-1} Cd, and 1000 mg kg^{-1} As. Given that sphalerite is usually the most important host mineral for cadmium in hydrothermal mineral deposits, there is a high correlation (R = 0.75) between this element and Zn. On the other hand, despite being two metallogenically intertwined elements in ore deposits, Pb and Zn show a less significant relationship, which can be attributed both to heterogeneities in the mineralogical composition of the veins, and to the complex history of the mineral concentration process: In the older process, the interest was only for Pb, meanwhile in the late period, the interest was focused in Zn. The Phytotoxkit® bioassay showed that soils with high PTEs presented very high toxicity, particularly the inhibition germination is related to Pb, As, and Cd content and root inhibition with Pb content. Both indexes were correlated with pH and electrical conductivity; samples with lower pH and higher soluble salt content are those with higher seed germination inhibition and root growth inhibition. On the other hand, the Ostracodtoxkit® bioassay showed very high sensitivity, with 100% mortality. The applied bioassays confirmed the soil toxicity and it is highly recommended to complement the results from environmental chemistry with results from bioassays, in order to provide a more complete and relevant information on the bioavailability of contaminants and to characterize the risk of contaminated areas.

Keywords: potentially toxic elements; water extraction; soil contamination; mining activities; mobility indicators; bioassay; bioavailability

1. Introduction

Sites where metal ores are mined or processed are potential sources of environmental pollution. In ancient mining districts, with long histories of mining and metallurgical activity, mine wastes represent one of the main sources of pollution for soils, water, air, and biota [1]. Acid mine drainage (AMD) from sulfide-rich waste-dumps exposed to weathering processes is an important focus of environmental impact [2,3], generally due to their low pH, high salinity, and high potentially toxic element (PTE) content.

Characterization of soil contamination by PTEs could not only be based on the determination of total contents, because it only provides limited information on the chemical behavior in terms of biological availability, potential toxicity, and mobility, but not in the possibility of affecting waters and biota. Therefore, good knowledge of the soil contamination and the assessment of the potential effect of soils polluted by PTEs require identification of the geochemical phases in which the elements are bound and the evaluation of metal retention and bioavailability [4].

To determine the degree of contamination of heavy metals in the soil, researchers employ various factors and indices like contamination factor (CF) [5], enrichment factor (EF) [6], or potential contamination index (Cp) [7].

Furthermore, the determination of the contaminants contents is not enough to fully evaluate the toxic effects or to characterize contaminated sites, because the ecotoxicological danger in the biota of the environment is not reflected, and no information is provided on the effects of the chemical compounds. To properly estimate the environmental risk of contaminants, chemical methods need to be complemented with biological procedures. Chemical methods provide information about metal availability, but to acquire data about metal bioavailability, biological environmental compartment must to be taken in account. Biotests can measure bioavailability of contaminants and the effects of the toxic compounds (chemically not measured) on the members of the soil biota. Therefore, ecotoxicological testing may be a useful approach for assessing the toxicity as a complement to chemical analysis [8].

Thus, a chemical and mineralogical characterization of the San Quintín West soils, together with the results of the simple chemical extraction of these soils, follows. Additionally, the application of mobility indicators allows us to explore the degree of PTEs contamination and the use of a battery of biotests allows for determining the magnitude of adverse effects in relation to living organisms from different trophic levels.

Previous environmental studies in the area [9–12], mainly described the inorganic compartments of the local environment; the present study is the first including the biological effects of the soil pollution.

2. Studied Area

The San Quintín Mining Group (Figure 1) is part of the so-called Alcudia Valley Mining District (AVMD) [13]. It is located within the so-called Meseta Sur (the Spanish southern mesa), which has a continental Mediterranean climate with contrasted seasonal variations in mean temperatures: 6–8 °C (winter) and 26–28 °C (summer). The rain concentrates in late autumn and early spring, with an annual total of 500–700 mm. The mining group is located within a region morphologically characterized by WNW trending valleys and sierras, within a landscape ranging in altitude 600–700 m above sea level.

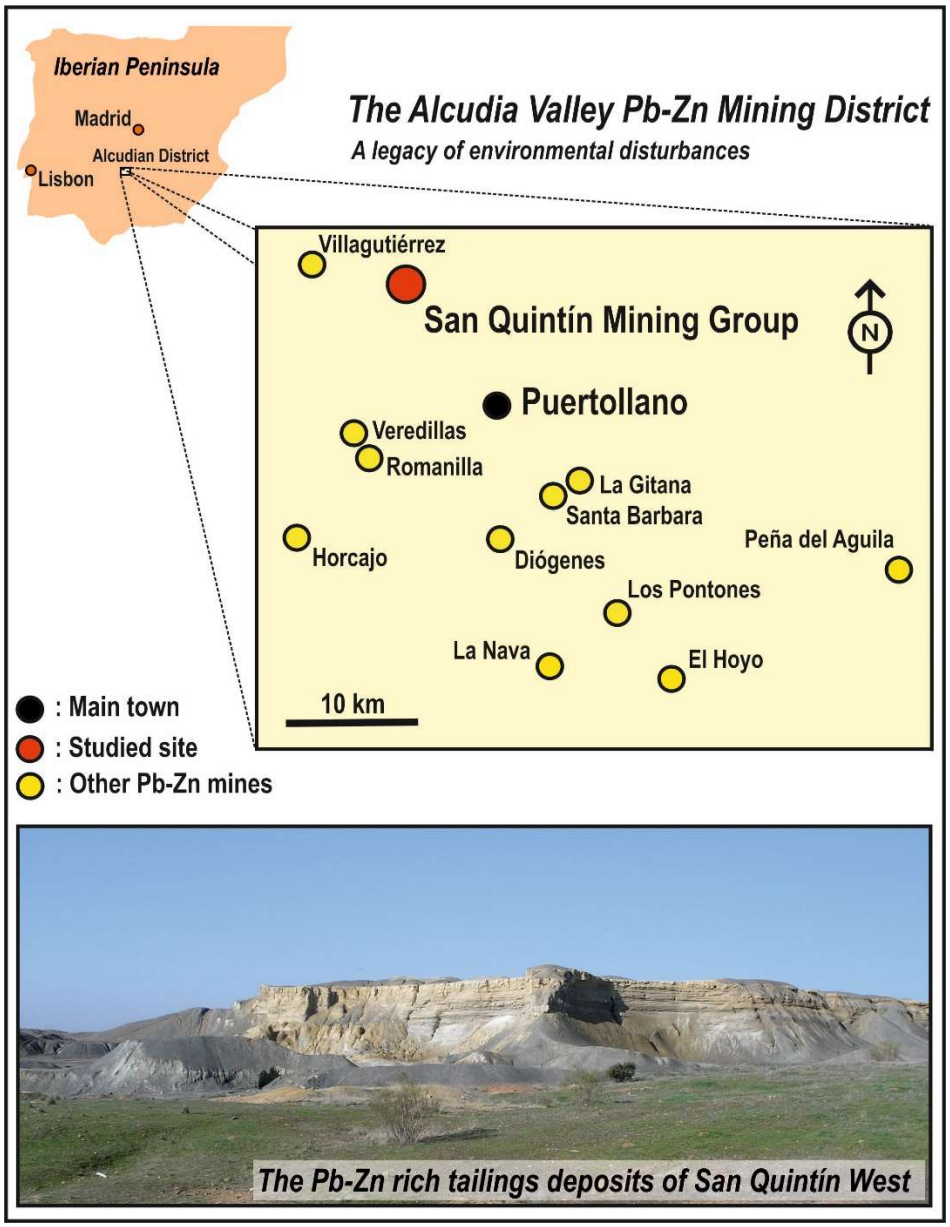

Figure 1. Location of the San Quintín Mining Group and the Alcudian Mining District in the Iberian Peninsula, and general view of the tailings deposits from San Quintín West.

The main soils are entisols, with localized development of anthrosols. Entisols are soils of recent origin, developed on unconsolidated parent materials with usually no genetic horizons except an A horizon. Anthrosols are soils that form or are profoundly modified through human activities, such as the addition of wastes. Other local soil-like materials include spolic technosols (recent deposits of artificial origin [14]), which, in the AVMD, appear related to abandoned tailings deposits in many mine sites.

This realm hosts the Alcudia Valley Mining District (AVMD) (Figure 1), which covers a large area of more than 1500 km^2; most of the ore deposits (now abandoned) were Pb–Zn–Ag veins. Most of them were very small but a few, such as San Quintín (500,000 t of Pb metal), El Horcajo (300,000 t of Pb metal), and Diógenes (200,000 t of Pb metal) (Figure 1) were important producers [13]. From a mineralogical and chemical point of view, a major problem regarding the AVMD (Figure 1), and particularly at San Quintín, relates to the important volume of tailings deposits. Tailings, if rich in pyrite (as it is the case at San Quintín), can be an active source of acid mine drainage (AMD). Oxidation of pyrite will, in turn,

greatly increase metal mobility from other sulfides, such as sphalerite and galena. In this regard, given the Mediterranean climate of the region, instead of a permanent flow of AMD, what usually forms at San Quintín area is a seasonal small stream of deep red to orange-colored waters (Figures 2 and 3).

Figure 2. San Quintín East and West depicting location of the "older" (1888–1923) and "modern" tailings (1973–1988).

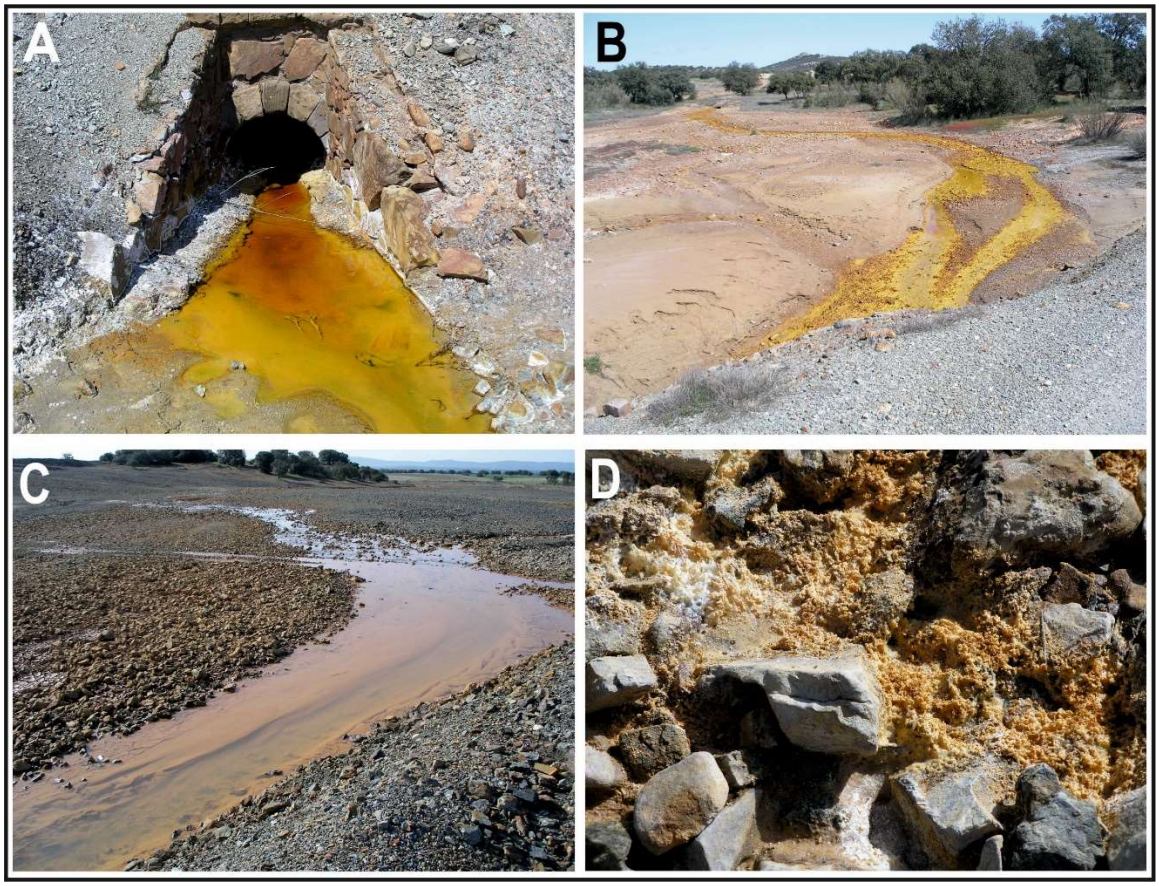

Figure 3. Acid mine drainage from San Quintín East (**A**,**B**) and near neutral mine drainage from San Quintín West (**C**,**D**).

The mining group is composed of two mining zones, separated by 800 m: San Quintín East (affecting an area of 12 Ha) and San Quintin West (affecting an area of 40 Ha).

The San Quintín Mining Group (East and West) (Figure 2) was active between 1888 and 1923 when about 515,000 tons of galena concentrates were produced (by gravity concentration with the aid of primitive jigs). Subsequently, between 1973 and 1988, the *Sociedad Minero-Metalúrgica de Peñarroya España* carried out a second mineral recovery operation of the old tailings (this time using froth flotation), estimated at around 3 million tons, with high Zn contents, a metal with hardly any interest at the time of the older exploitation. However, this operation did not affect the tailings left at San Quintín West (Figure 2), where our research was centered. From the older period, there are many waste dumps of barren rock whose environmental risk is low, thus, the main hazard relates to the tailings, which in this case, are constituted by residues of concentration of minerals by gravity, a process that was inefficient at the time and left behind residues very rich in galena (PbS) and sphalerite (ZnS). These old and chaotic tailings deposits are a separate case and present a significant environmental hazard by heavy metals (Pb, Zn–Cd) and metalloids (As). These tailings do not only contain high concentrations of Pb and Zn (up to 48,600 ppm Pb and 34,000 ppm Zn), but also are a source of acid mine drainage (AMD).

3. Sampling and Analysis

3.1. Sampling

To assess the potential hazards derived from having metal and metalloid rich abandoned tailings deposits, we studied San Quintín West side of the old mineral recovery operations (Figure 2). We made this decision because different from the eastern side, this sector only hosted tailings generated during the 1888 and 1923 period, thus the mixing of older and newer tailings materials in the artificial soils was prevented. We took 33 samples from the San Quintín West technosols [14], that is, recent (e.g., less than 100 years old) soil-like deposits of artificial origin such as the erosion of tailings deposits in our case [12]. Given that the topsoil is the most important part of the soil profile for degradation control, we concentrated our efforts on this superior horizon (5 to 30 cm in our sampling). Soil samples were collected with a shovel in each subplot, then mixed and homogenized.

In order to establish background values, three soil samples were collected in an unaffected area, in the surroundings of the mining area. Unaffected samples were previously chosen taking into account the mining district limits, soil and water dispersion, and other anthropogenic sources.

3.2. Chemical and Mineralogical Analysis

All samples were air-dried and sieved through a 2 mm mesh. The pH and electrical conductivity (EC) were determined in a 1:5 (w/v) suspension of an aliquot of soil in pure, deionized water (Milli-Q; resistivity $\geq$ 18.2 MΩ).

To determine the total PTEs content, the soils were first ground to a fine powder using a zirconium ball mill. Aliquots (0.1 g) of soil samples were placed in Teflon vessels, and a mixture of 5 mL concentrated HF (37%), 0.2 mL concentrated HNO_3 (65%), and 5 mL of water was added. After digestion in a conventional microwave oven, the solutions were transferred to a volumetric flask, brought to 50 mL, and analyzed.

The samples were subjected to a leaching test, according to standard UNE-EN-12457 [15]. The UNE EN 12457-4 test is an extraction method with distilled water, in a liquid-to-solid ratio of 10 for 24 h. Water extraction was used to assess the natural mobility of PTEs under actual conditions, simulating the effect of rainfall in the studied materials.

Extraction from soil samples were analyzed using inductively coupled plasma-optical emission spectrometry (ICP-OES) (SPECTRO ARCOS, Kleve, Germany) for quantification of As, Cd, Pb, Zn, and Fe levels. Quality control and assessment was done by analyzing duplicate samples to check precision. Accuracy was obtained by using the certified standards (NCS DC 73319, NCS DC 73320, NCS DC

73321, NCS DC 73323, NCS DC 73324, NCS DC 73325). RP of the different elements range from 82% to 110% and the RSD was <6%.

The mineralogy was defined through X-ray diffraction (XRD). Original soils and residues after the water extraction were ground in an agate mortar and sieved through a 53 µm mesh. Mineral phases were identified by powder XRD using a Philipps Analytical PW 1752 Cu Kα radiation power diffractometer (Philipps Analytical, Almelo, The Netherlands), fitted with graphite monochromator radiation $K\alpha_1$ = 1.5406 Å. Diffractograms were recorded continuously at 2θ angles from 2° to 68°, with 0.02 stepping intervals and 1 s per step. The semiquantitative analysis was carried out according to the Chung method [16,17], using XPowder software (Ver 2010.30.01). The Chung method is based on the determination of the reference intensity ratios (*RIR*) of the existing phases, which allows the intensity calculations to be normalized on the statement that the sum of all phases in the sample is equal to 100%.

3.3. Geochemical Indicators

A significant number of indicators designed to evaluate the quality of soils can be found. Contamination level of selected heavy metals was assessed by single factor contaminant index (*PI*) and pollution load index (*PLI*) using Equations (1) and (2) [18].

$$PI = \frac{C_{soil}}{C_{background}} \quad (1)$$

$$PLI = (PI_{Pb} \times PI_{As} \times PI_{Cd} \times PI_{Fe} \times PI_{Zn})^{\frac{1}{5}} \quad (2)$$

where *PI* is the single factor pollution index of each metal and C_{soil} and $C_{background}$ are the concentrations of metal in the soil sample and background, respectively (mg kg^{-1}). $PI < 1$ (non polluted); $1 \leq PI < 2$ (slightly polluted); $2 \leq PI < 3$ (moderately polluted); $PI \geq 3$ (highly polluted).

PLI is pollution load index and n is the number of pollutants assessed (five in our study). *PI* is the single factor pollution index of each metal: $PLI < 2$ (moderately to unpolluted); $2 \leq PLI < 4$ (moderately polluted); $4 \leq PLI < 6$ (highly polluted); $PLI > 6$ (very highly polluted).

3.4. Mobility of Potentially Toxic Elements (PTE)

Similar to total PTEs contents, indicators for water extraction were established in order to evaluate the mobilization of potentially toxic elements. The natural mobility of PTEs was studied by water extraction and represents the soluble fraction. Natural mobility indicators for lead ($NMIn_{Pb}$), arsenic ($NMIn_{As}$), cadmium ($NMIn_{Cd}$), iron ($NMIn_{Fe}$), and zinc ($NMIn_{Zn}$) were calculated as the ratio between the PTEs concentrations with its background values after the water extraction:

$$NMIn_n = \frac{C_{sample\ after\ water\ extraction}}{C_{background\ after\ water\ extraction}}$$

The natural mobility index (*NMI*) has been determined as the *n*th root of the product of the *n* natural mobility indicators. In our case:

$$NMI = (NMIn_{Pb} \times NMIn_{As} \times NMIn_{Cd} \times NMIn_{Fe} \times NMIn_{Zn})^{\frac{1}{5}}$$

Indicator values lower than 2 points to low mobility; values from 2 to 4 suggested moderate mobility; from 4 to 6, considerable mobility; and higher than 6 is evidence of very high mobility [19].

3.5. Toxicity Tests

Ecotoxicity was investigated by means of a set of bioassays composed of two microbiotests using four test organisms.

3.5.1. Seed Germination Bioassay

The phytotoxicity of the sediment samples was evaluated using the Phytotoxkit microbiotest, provided by Microbiotests Inc. (Gent, Belgium), Belgium. The Phytotoxkit® test measures the decrease in (or the absence of) seed germination and of the growth of the young roots after 3 days of exposure of seeds of selected higher plants to a contaminated matrix compared with the controls germinated in a reference soil.

When evaluating toxicity in plant species, it is highly advisable to use both monocotyledonous and dicotyledonous species [20]. Then, the plants selected for the Phytotoxkit microbiotest were: The monocotyl *Sorghum saccharatum* (Sorgho); and the dicotyls *Lepidium sativum* (Garden cress) and *Sinapis alba* (mustard). The tests were performed essentially as described in the Phytotoxkit protocol [21]. Ten seeds of each plant were placed at equal distance near the middle ridge of the tests plate on a black filter paper placed on reference soil (control) or sediment samples and hydrated with deionized water. The plates were placed vertically in a holder and incubated for three days at 25 °C, in darkness. Pictures of the test plates at the end of the exposure period were taken and the length of the root of each plantlet was measured using CMEIAS-IT version 1.28 (MSU Center for Microbial Ecology, East Lansing, MI, USA) [22].

The percent inhibition of seed germination (*IG*) and inhibition of root growth (*IR*) for the plant were calculated using:

$$IG \text{ or } IR = \frac{A - B}{A} \times 100 \text{ percent}$$

where A is the mean seed germination or root length in the control (mm); and B is the mean seed germination or root length in the test sediment (mm).

3.5.2. Ostracod Toxicity Test

Ostracodtoxkit F™ is the best known and first biotest for direct contact of crustaceans with freshwater and brackish samples. Unlike bacteria, ostracods have a fully developed gastrointestinal tract, through which toxic substances can enter an organism (easily bioavailable pollutants can also enter via body shells and gills). Toxicity tests using the benthic ostracod, *Heterocypris incongruens*, were conducted according to the manufacture's instruction [23]. Effects on the organism were determined after 6 days of direct contact with freshwater sediments. In brief, cysts of the ostracod were hatched 52 h before each test, and 10 neonates were added to each of three wells containing a mixture of 1 mL of solid sample, 2 mL of synthetic freshwater, and 2 mL of algal suspension. After 6 days of exposure at 25 °C in darkness, the toxicity was evaluated as mortality of the ostracod. Test acceptability required that the mean mortality of the ostracod in the control sample with the reference sediment provided in the kit should be less than 20%, and the mean growth in body length of the ostracod in the reference sediment should be at least 400 µm.

Growth inhibition (*GI*) of *H. incongruens* was calculated:

$$GI = 100 - \frac{C}{D} \times 100 \text{ percent}$$

where C is the increment of the ostracods in the reference OECD soil and D the increment of the ostracods in the investigated substrates.

The system of toxicity classification developed by Persoone et al. [24] was used to estimate the soil toxicity: *PE* (percent toxic effect) < 20%, no significant toxic effect, class I, no acute hazard; 20% < *PE* < 50% significant toxic effect, low toxic sample, class II, low acute hazard; 50% < *PE* < 100% significant toxic effect, toxic sample, class III, acute hazard; *PE*-100% (single test), class IV, high acute hazard; *PE*-100% (all tests), class V, very high acute hazard (Table 1).

Table 1. Hazard classification system for bioassays.

Percent Toxic Effect (*PE*)	Class	Hazard
≤20%	Class I	No acute hazard
20% ≤ *PE*< 50%	Class II	Slight acute hazard
50% ≤ *PE*< 100%	Class III	Acute hazard
PE 100% in at least one test	Class IV	High acute hazard
PE 100% in all tests	Class V	Very high acute hazard

3.6. Geostatistical Analysis

To deal with extremely variable concentration data (up to four orders of magnitude), we also dealt with the information transforming our dataset to log10(x) in order to dampen these extreme variations; geometric means were calculated in this case. To deal with the array of geochemical data, we used the STATGRAPHICS Centurion XVII package (Statgraphics Technologies, The Plains, VA, USA) to: (1) Calculate regression lines and correlation coefficients between pairs of elements; (2) clustering analysis, building a dendrogram (clusters by group average; distances: Squared euclidean), aimed to identify related groups of variables; (3) we also run a principal components analysis (PCA) for the identification of underlying patterns in our data, to highlight similarities, differences, and trends; and last but not least, (4) we finally did kriging to estimate values at locations with no sampling (e.g., [25]), mostly to identify 2D spatial distribution patterns for the different variables.

The spatial distribution of PTEs was displayed using kriging spatial interpolation technique in Surfer 13.

4. Results and Discussion

4.1. Mineralogy and Geochemistry of Soil Samples

Table 2 shows the results of geochemical analyses, including the elements Pb, Zn, As, Cd, and Fe, together with some reference values, and including the analysis of a local reference sample ("Blanco"), which location is also shown in Figure 1, 250 m south of the affected area.

All samples showed acidic pH, ranging from 2.1 to 6.3. Samples S22, S23, and S25 showed the lowest values, 2.1, 2.3, and 2.2 respectively. These samples are characterized by high electrical conductivity values, ranging from 7.1 to 9.5 mS cm^{-1}. Except for "Blanco" soil, all collected materials are characterized by pH values lower than 5 (58% of samples). With regards to the EC values, 60% of soil samples showed EC values above 2 ms cm^{-1}. Only some sampling points (S4, S5, S13, and S27) showed EC values lower than 1 mS cm^{-1}, suggesting that soluble salt content is high in San Quintín mining district.

As expected, the mean concentrations (either arithmetic or geometric means) are extremely high, and only comparable to analogous cases from other abandoned Pb–Zn tailings elsewhere in SE Spain (Table 2).

Average Pb, Zn, and As concentrations are respectively 1000, 250, and 6.5 times higher than the regional background levels established by Bravo et al. [28] for Castilla-La Mancha region; average Cd is 4.5 times higher than regional background established by Jiménez-Ballesta et al. [26] also for the Castilla-La Mancha region. All these values are also well above the reference levels, defining the need to apply a risk assessment procedure in order to determine and quantify potential risks both to human health and to ecosystems.

Table 2. Main statistics of geochemical values. CLM-B and CLM-RL: Background values for Castilla-La Mancha region, *: After Jiménez-Ballesta et al. [26]; **: after Bravo et al. [27]. Means and geometric means (*italics*) for the San Quintín West spolic technosols, and equivalent materials from abandoned Pb–Zn mining sites in SE Spain. We also calculated the geometric mean as different from the arithmetic mean as it dampens the statistical effect of very high or low values; this procedure was not required in the case of iron.

Element (mg kg^{-1})	Pb	Zn	Cd	As	Fe	Reference
San Quintín West (SQW)						
Mean	18,036	8825	38	88	42,597	This work
Geometric mean	12,177	5408	10	16		
Standard deviation	13,409	8075	35	226	33,943	
Minimum	1000	340	1	1	10,500	
Maximum	48,600	34,200	200	1000	166,900	
Blanco	600		1	11		
Background values Castilla la Mancha						
CLM-B	17.9	35.0	3.9 **	6.5	XX *	** Bravo et al. [27] * Jiménez-Ballesta et al. [26]
CLM-RL	27.1	57.2	4.4 **	14.1	XX *	
Other Pb-Zn mining sites in SE Spain						
Cabezo Rajao (soils & mine wastes)	8000	12,500	41	315		Navarro et al. [28]
Mazarrón District (tailings)	12,401	6101	15	654		Oyarzun et al. [29]
	10,304	*5120*	*12*	*497*		Oyarzun et al. [29]

The key resides in the volumetrically importance of pyrite (FeS_2) and the release of Fe^{3+}. If pyrite is important (as in San Quintín) (3) then (e.g., [29]):

$$4FeS_2 + 14O_2 + 4H_2O \leftrightarrow 4FeSO_4 + 4H_2SO_4 \quad (3)$$

$$4FeSO_4 + 2H_2SO_4 + O_2 \leftrightarrow 2Fe_2(SO_4)_3 + 2H_2O \quad (4)$$

$$Fe_2(SO_4)_3 \leftrightarrow 2Fe^{3+} + 3SO_4{}^{2-} \quad (5)$$

The chemical evolution of the system from (3) to (5) is the main prerequisite to induce oxidation and hydrolysis of galena (6) and sphalerite (7) (Oyarzun et al., 2011 [29]):

$$PbS + 8Fe^{3+} + 4H_2O \leftrightarrow Pb^{2+} + 8Fe^{2+} + SO_4{}^{2-} + 8H^+ \quad (6)$$

$$ZnS + 8Fe^{3+} + 4H_2O \leftrightarrow Zn^{2+} + 8Fe^{2+} + SO_4{}^{2-} + 8H^+. \quad (7)$$

However, given that sphalerite often contains Cd, we may express the oxidation and leaching of this metal in the following way (8):

$$Zn_{1-x}Cd_xS + 8Fe^{3+} + 4H_2O \leftrightarrow (1 - x)\ Zn^{2+} + xCd^{2+} + 8Fe^{2+} + SO_4{}^{2-} + 8H^+. \quad (8)$$

Lead and zinc form one of the classic associations in ore deposits, and in this regard, galena and sphalerite are their most common sulfide minerals [30].

We found some remarkable relationships between the studied variables. For example, there is a clear relationship between Zn and Cd (Figure 4A) (R = 0.75; *P*-Value: 0.0000: Significant relationship). These elements belong to the same group of the periodic table (IIB) and share chemical properties such

as the tetrahedral covalent bond and other crystal structures. They have relatively similar ionic radii (Pauling): Zn^{2+} (0.74 Å) and Cd^{2+} (0.97 Å), which accounts for the observation that cadmium occurs in sphalerite as an isomorphous impurity [31]. Thus, the main host mineral for cadmium in lead–zinc ore deposits is sphalerite, and cadmium content in this mineral depends on the type of deposit [30]. Pb–Zn are also significantly related, although the connection is weaker than the Zn–Cd relation (R = 0.56; *P*-Value = 0.0008). This is also well depicted by the cluster analysis, with the dendrogram showing a neat Zn–Cd group while Pb is related to this pair at a lesser extent, meanwhile As constitutes a differentiated variable on its own (Figure 4C). The same tendencies can be observed in the PCA (Figure 4D,E) and in the kriging maps of Zn, Cd, and Pb (Figure 5), which display similar tendencies, particularly for Zn and Cd.

On the other hand, the numerically excellent correlation between As and Fe (R = 0.89) may be somewhat misleading, as it is strongly influenced by a few outliers (high Fe and As samples), thus defining what could be regarded as a "normal" (background) population and an anomalous one (Figure 4B). However, this is a case that has to be closely examined because the kriging maps of As and Fe show relatively similar spatial tendencies (Figure 5). Arsenite and arsenate have a strong sorption affinity for iron hydroxide and oxyhydroxide minerals such as ferrihydrite and goethite [32]. Colloidal goethite (FeO(OH)) has a net positive charge [33] in acid media, which binds arsenic complex ions by adsorption. However, these complex ions may remain strongly bound to goethite up to higher pH values of 8.0–8.5 [34,35]. Desorption of arsenic from goethite may occur by competition between negative charges for the positive colloid, a reduction of the iron oxide mineral phase [36], or high pH values (>8.5). Given the Eh–pH conditions of the superficial environment of San Quintín West we may rule out the second and third possibility. In this regard, as indicated by O'Day [33], under fully oxidized conditions, arsenate binds strongly to Fe^{3+} oxide minerals as an inner-sphere complex. Except for the cluster analysis (there were no clear relationships between As and Fe), both the PCA and kriging maps show significant relationships for these two elements. The angle between vectors (cosine of the angle) in PCA approximates the correlation between the variables they represent; that is, the closer the angle is to 90° or 270°, the smaller the correlation, whereas an angle of 0° or 180° reflects a correlation of 1 or −1, respectively [37]. In this respect, Zn and Cd are almost collinear and Pb shows the same similar tendency in what we have defined as cluster (group) 1, stressing the relationships between these elements (Figure 4D). In this figure, As appears as an isolated variable; however, if Fe is introduced to the PCA, a new cluster (2) grouping of As and Fe appears (Figure 4E). Because the only relevant iron oxide phase present in San Quintín West is goethite, we may assume that As is somehow bound to this mineral.

The semiquantitative mineralogical composition is summarized in Table 3. All samples showed similar mineralogical composition, consistent with what would be expected in an area affected by lead sulphide mining. Soils showed varying percentage of phyllosilicates, feldspar, quartz, gypsum, plumbojarosite, anglesite, alunite, goethite, hematite, and amorphous minerals.

With regards to the results obtained, soils with higher concentrations of target elements (S25, S22, S20) have the higher contents of plumbojarosite. In addition, samples whose Pb concentration is high but not presented high plumbojarosite content, are characterized by high anglesite contents, such as S23. On the other hand, samples with lower concentrations of the studied elements are characterized by the presence of phyllosilicates, and with lower proportions of plumbojarosite and anglesite.

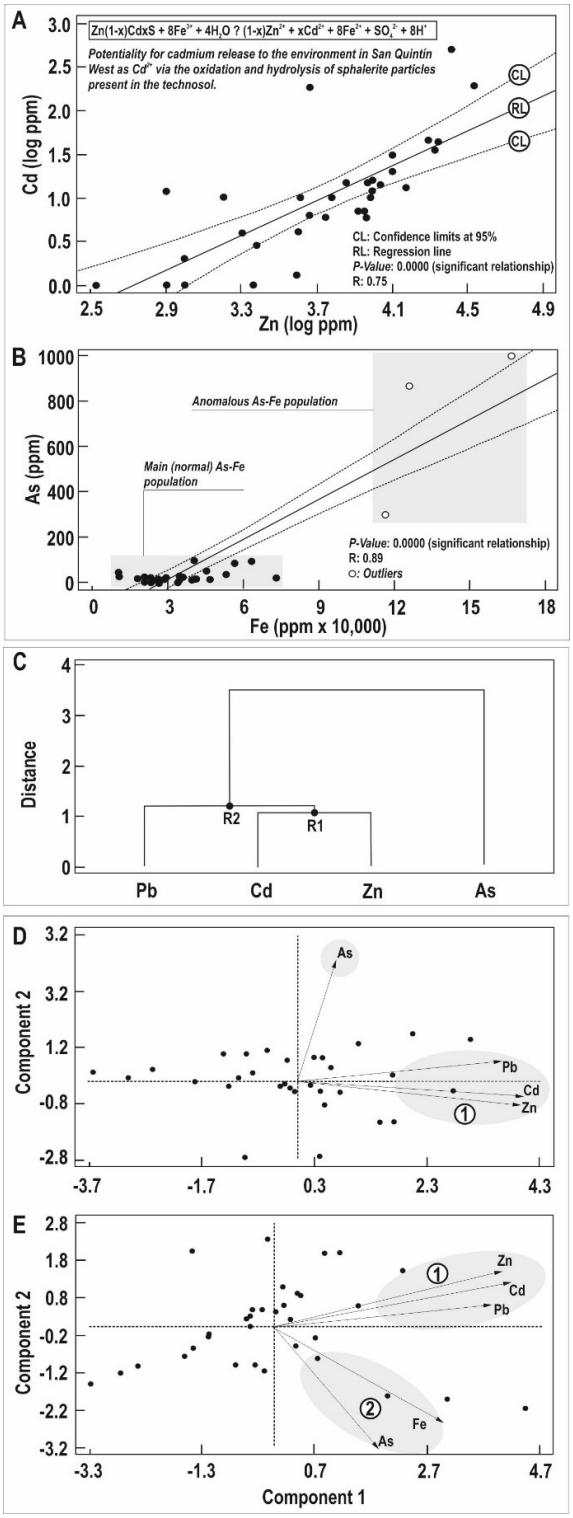

Figure 4. Regression lines and statistical data for the Zn–Cd (**A**) and Fe–As pairs (**B**); note the existence of normal and anomalous populations in (**B**), which may be indicating that the high correlation (0.89) is probably inexistent. (**C**) Clustering analysis and resulting dendrogram (clusters by group average; distances: Squared euclidean) for Pb, Zn, Cd, and As. (**D**) Principal components analysis (PCA) for Pb, Zn, Cd, and As; first, main component: 0.541581 × log Pb + 0.0997684 × log Asc + 0.594177 × log Cd + 0.586251 × log Zn, second component: 0.167213 × log Pb + 0.958876 × log As − 0.121497 × log Cd − 0.194514 × log Zn. (E): PCA for Pb, Zn, Cd, As, and Fe; First, main component: 0.381289 × Fe + 0.495067 × log Pb + 0.235753 × log As + 0.53719 × log Cd + 0.515146 × log Zn; second component: −0.552223 × Fe + 0.134644 × log Pb − 0.707019 × log As + 0.263836 × log Cd + 0.327771 × log Zn. All statistics calculations run with STATGRAPHIC Centurion XVII (Statgraphics Technologies, The Plains, VA, USA).

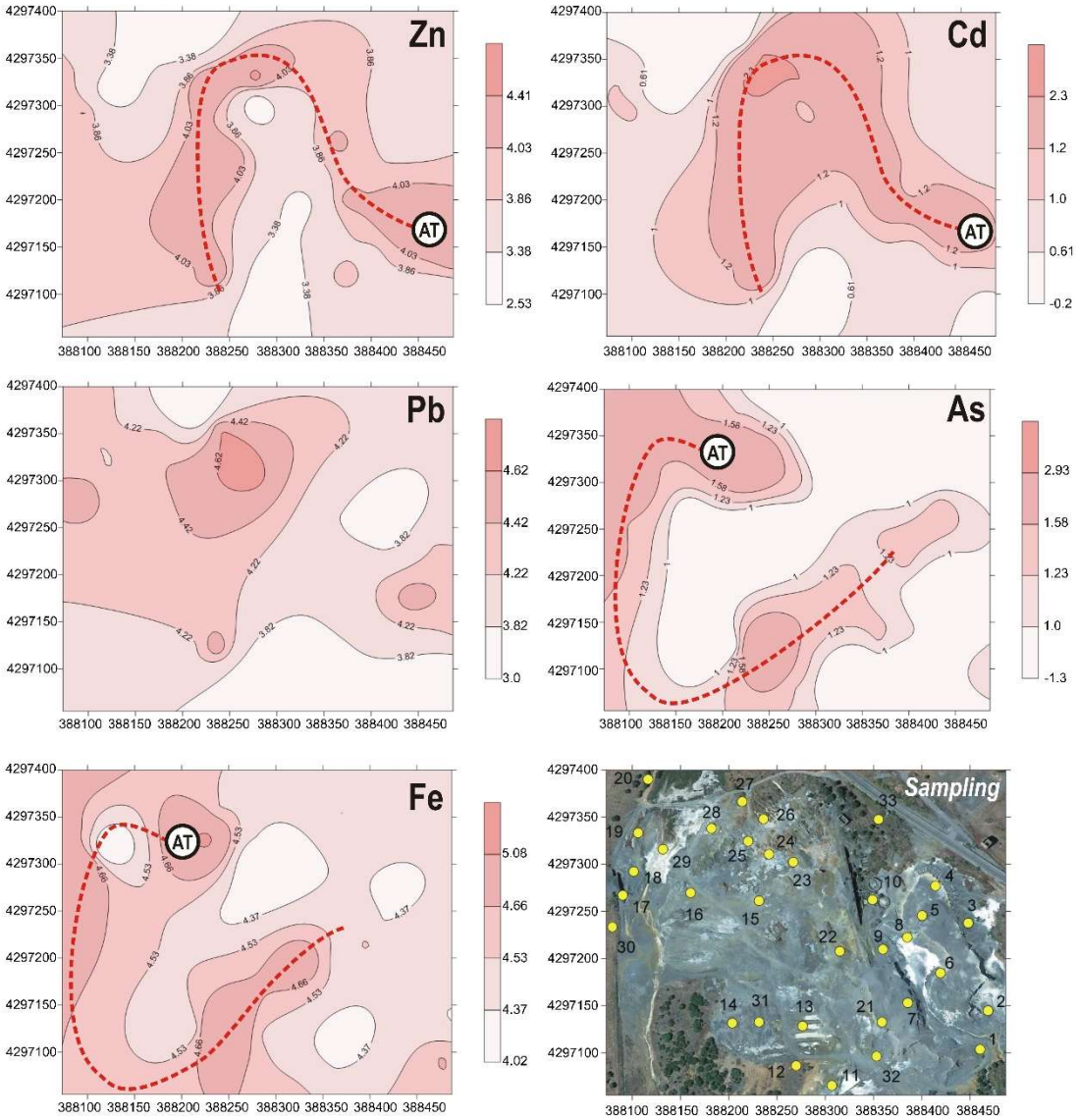

Figure 5. Kriging maps for Zn, Cd, Pb, As, Fe, and sampling location map. AT: Axial trend of the anomalies. Graphics: STATGRAPHIC Centurion version XVII. Note the striking spatial similarities of trends for the Zn–Cd and As–Fe pairs.

The pollution index (*PI*) showed the highest values for Cd (average of 36), lead (29), and zinc (24). On the other hand, Fe showed the lowest *PI* values (average of 2) and arsenic showed a mean value of 8 for selected samples. With regards to the CF results for Pb, Cd, and Zn, almost all samples showed values above 3, with very high values in S24, S25, and S26 soil samples. On the other hand, the lowest values have been quantified in points S11, S12, and S13. The results of the *PI* for As show a maximum at point S25. For the rest of the samples, *PI* values are low, in many cases less than one. For the case of Fe, only two points (S25 and S31) show very high contamination, with values above 3. The rest of the points are characterized by a moderate contamination. A total of 94% of samples are highly contaminated for Pb, 79% for Zn and Cd, and 27% for As. Only 15% of samples showed *PI* higher than 3 for Fe.

Table 3. Mineralogical composition (%) of soil samples.

	Phyllosilicates	Feldspars	Quartz	Gypsum	Plumbojarosite	Anglesite	Alunite	Hematite + Goethite	Amorphous
S1	28	12	31	6	3	2	3	10	6
S2	22	17	29	8	3	3	8	6	5
S3	18	10	22	15	6	3	9	11	6
S4	27	20	41	0	2	2	3	2	4
S5	33	18	36	0	1	1	3	3	4
S6	18	12	19	11	6	5	14	9	6
S7	27	17	25	7	3	3	7	5	5
S8	19	9	29	15	12	2	5	5	5
S9	26	12	32	8	2	3	8	6	4
S10	22	15	29	9	4	3	7	6	5
S11	11	8	11	36	20	0	2	4	9
S12	21	16	31	8	3	2	4	10	6
S13	21	14	30	9	4	3	9	7	5
S14	25	12	30	8	4	3	8	7	5
S15	20	14	23	11	3	4	11	9	6
S16	23	14	23	8	9	3	7	6	6
S17	19	11	16	0	30	2	6	7	9
S18	10	8	9	3	50	2	5	5	10
S19	18	10	25	6	27	2	3	4	6
S20	16	11	22	5	26	2	5	7	7
S21	31	12	41	4	1	2	2	4	4
S22	14	13	25	6	24	2	5	5	7
S23	9	15	10	6	0	10	26	14	9
S24	20	13	19	9	4	5	14	8	7
S25	5	7	2	2	68	1	2	4	9
S26	13	19	13	7	5	6	17	12	8
S27	18	4	58	0	4	0	0	12	3
S28	14	7	15	10	41	1	1	4	7
S29	14	14	36	9	12	3	0	7	4
S30	21	19	21	3	22	1	0	5	7
S31	9	7	4	8	53	3	3	5	10
S32	22	10	42	12	4	2	0	5	4
S33	21	12	41	0	8	2	3	9	4

Considering all the elements, the *PLI* results indicate that only six sampling points reached moderately contamination (S1 and S13) or are classified as unpolluted (S12, S26, S32, and S33). On the other hand, maximum values for this index are found in S30 with a $PLI = 69$. Samples with $PLI > 3$, and classified as highly contaminated, represented the 55% of total sampling points.

Almost all samples from San Quintín showed very high pollution load index for selected elements and total contents. Therefore, a risk assessment procedure has to be carried out in the area, aimed to study if present hazards could pose a risk to human health or to ecosystems.

4.2. Mobility of PTEs

The water-extractable PTEs contents (Table 4) showed a wide variation range. Average soluble Pb content was 4.95 mg kg^{-1}, reaching a maximum value of 22.5 mg kg^{-1} in S29, followed by S28, S30, and S31. Even if in these samples some lead has been mobilized, the extraction percentage is low, with values below 0.5% in all samples. The average percentage extraction was 0.04%, and the low standard deviation suggests that all samples showed similar behavior after this extraction for Pb.

Table 4. Mean potentially toxic element (PTE) content and extraction percentage after the selective extraction.

	Pb	As	Cd	Fe	Zn
Mean (mg kg^{-1})	5	3	19	1856	<dl
Extraction %	0.04	19	39	7	<dl

<dl: below the detection limit.

The soluble As content was also determined and only two soil samples showed values higher than the detection limit: In sample S22, 0.22 mg kg^{-1} was determined for this fraction, while in sample S24, the concentration was of 6 mg kg^{-1} (Table 4). Considering the total content, the extraction percentage was calculated, and it showed that in S24, 37% of the arsenic is mobilized under these conditions, while in sample S22, this percentage was only 0.5%.

Cadmium showed the highest variability regarding the water extraction, with an average value of 19 mg kg^{-1} and a maximum of 300 mg kg^{-1}, determined in sample S25. Samples S24, S26, and S31 showed values above average value. The samples with the highest concentration of soluble Cd are located in the north of the study area, except the sample S31. With regards to the extraction percentage, S24 showed 17%, while samples S25 and S26 showed values of 60% and 70%, respectively. Samples such as S29, S31, S2, and S11 showed extraction percentages of almost 100%, suggesting that this element could be easily mobilized by rainfall episodes.

Soluble Fe contents showed strong differences among analyzed samples. In points such as S20, S21, S22m and S23, values ranged between 4225 and 9950 mg kg^{-1} respectively. Other samples, such as S12, S16, S26, or S31 showed Fe much lower contents, ranging from 44 to 150 mg kg^{-1}. The rest of soil samples were under the detection limit for this element (Table 4). With regards to the extraction percentage, the highest value was found in sample S23, with 52%, followed by samples S21 (22%) and S22 (14%). The rest of the samples showed extraction percentages below 1%.

Taking into account all the elements, samples from S20 to S26 (Figure 5), together with S31, showed the highest soluble contents, suggesting that in this area there is a high mobilization risk under natural conditions, for example, after a rainfall episode.

The mineralogical composition after the water extraction suggested that samples present very small variations with respect to the original sample; only gypsum has been solubilized in a small quantity, except in sample S21, in which it was completely solubilized. The other mineralogical phases have not been affected.

The natural mobility indicator has been determined after the water extraction. All Zn mobility index values are below the detection limit, so the *NMI* of this element could not be calculated. Same as the rest of the points, almost all the samples have low contamination for As and Fe. Only point S24 has mobility index values higher than 6, so for these elements, the mobility is very low. On the contrary, the results showed that Cd and Pb have a very high natural mobility, with index values above 6 in most points.

Considering all the elements, only point S22 presents a high risk of natural mobility while in the rest, this risk is very low.

4.3. Bioassays Results

With regards to the ostracod bioassay results, the mortality of organisms in all samples is 100%, which indicates a very high sensitivity of these organisms to soils contaminated by PTEs present in this area. This experiment, therefore, showed that San Quintín mining area represents a high risk to ecosystems. Only in S33 the mortality was lower than 100%, with a value of 49%.

Phytoxkit results showed that, in general, the toxicity values are high, represented by a high percentage of inhibition in germination (Table 5).

Table 5. Phytotoxkit bioassay results.

	Germination Inhibition (%)			Root Inhibition (%)			Ostracodtoxkit	Class
	Ls	**Sa**	**Ss**	**Ls**	**Sa**	**Ss**		
S1	12	10	10	36	61	3	100	IV
S2	100	40	30	100	81	55	100	V
S3	10	10	10	29	40	51	100	IV
S4	20	20	30	44	15	39	100	IV
S5	0	10	10	0	0	2	100	IV
S6	100	100	95	100	100	87	100	V
S7	44	20	10	62	64	0	100	IV
S8	33	50	10	93	88	95	100	IV
S9	87	60	0	92	85	73	100	IV
S10	22	30	20	77	84	43	100	IV
S11	10	60	20	89	85	90	100	IV
S12	0	10	10	68	65	65	100	IV
S13	10	10	10	63	34	56	100	IV
S14	20	10	10	47	26	21	100	IV
S15	10	10	10	73	72	35	100	IV
S16	17	20	20	80	71	79	100	IV
S17	20	20	10	74	78	65	100	IV
S18	50	100	78	100	100	86	100	IV
S19	25	0	0	81	79	77	100	IV
S20	0	10	20	30	1	33	100	IV
S21	12	20	10	0	0	10	100	IV
S22	100	100	100	100	100	100	100	V
S23	100	100	100	100	100	100	100	V
S24	100	100	100	100	100	100	100	V
S25	100	100	100	100	100	100	100	V
S26	17	20	20	90	89	81	100	IV
S27	15	10	8	100	100	84	100	IV
S28	0	20	20	61	32	53	100	IV
S29	11	90	40	100	100	91	100	IV
S30	22	70	30	75	100	74	100	IV
S31	15	10	8	100	100	84	100	IV
S32	0	10	20	26	5	33	100	IV
S33 (Blanco)	0	0	0	10	0	36	49	II

Ls—*Lepidium sativum*, Sa—*Sinapis alba*, Ss—*Sorghum saccharatum*.

The average percentage of germination inhibition was 33% for *Lepidium sativum*, 38% for *Sinapis alba,* and 27% for *Sorghum saccharatum*. One hundred percent of germination inhibition for the three selected species was determined in samples S22, S23, S24, and S25. Mortality of 100% for *L. sativum* and *S. alba* was determined in S6, while for *S. saccharatum* this value was 40%. *S. saccharatum* is a monocotyledonous species, so it is possible that this lower sensitivity is related to characteristics of the

species [20]. In the same way, S2 showed 100% of germination inhibition for *L. sativum*. Both S2 and S6 have high Pb and Cd content.

Samples S22, S23, S24, and S25 are those that showed low pH, with values lower than 3. In addition, these soils have high PTEs content, above the reference values of the studied area. S25 showed the highest content for As. The reference values for As were 16.1 mg kg^{-1}, 4.4 mg kg^{-1} for Cd and 44.2 mg kg^{-1} for Pb [27].

The growth inhibition results showed that chronic toxicity is also high for the selected species; samples such as S2 showed growth inhibition close to 100% for *Lepidium sativum*, as well as S6, S18, and S29 for *Lepidium sativum* and *Sinapis alba* and S22, S23, S24, and S25 in the three species studied.

On the other hand, samples S3, S4, S5, S20, S21, S32, and S33 showed growth inhibition percentage lower than 50%. These samples correspond to low soluble PTEs content and high pH values. The average percentage of growth inhibition for *Lepidium sativum* was 68%, 63% for *Sinapis alba,* and 59% for *Sorghum saccharatum*.

The data of potential toxicity were described using the system of toxicity classification proposed by Persoone et al. [24] (Table 1). The local reference sample ("Blanco") belonged to Class II. All soil samples to Classes IV and V. The highest toxicity (Class V) was detected in 5 samples, S2, S6, S23, S24, and S25 (Table 4). These samples are characterized by a very high soluble and total PTEs and acidic pH.

A Pearson correlation analysis was carried out (Table 6), considering the results of the geochemical characterization and indexes and those obtained after the toxicity tests.

Several relationships can be appreciated, among which the direct correlation between pH, EC, PTEs content, *NMI*, *PLI*, and plant toxicity results (both germination inhibition and growth inhibition percentage). Samples affected by acid mine drainage processes (with high PTEs and soluble sulphate content and low pH) are those with higher inhibition percentages. A positive correlation was found between PTES and germination inhibition and the three selected plant species for Pb and Cd. For Zn, As, and Fe content, a positive correlation was also found between the GI index for *S. saccharatum* and *S. alba*.

The increase in the content of Pb and Cd causes greater inhibition in the germination of the selected species; however, when the root inhibition percentage is evaluated, there is a relationship between Pb content and RI index of the species *Sinapis alba* and *Sorghum saccharatum*.

Finally, the zinc, arsenic, and iron content have direct relationships with the percentage of inhibition of the germination of the species *Sinapis alba* and *Sorghum saccharatum*, but not with the species *Lepidium sativum* or with the inhibition of root growth.

PLI index is positively correlated with PTEs content, reaching a Pearson value of 0.93 with arsenic and with the germination inhibition index of the three selected species. The geochemical indicators are also positively correlated with electrical conductivity and negatively with the pH.

The results of the bioassay on ostracods were not considered in the statistical analysis because all the samples, except one, had a 100% mortality.

Proposed bioassays have also been applied in other areas affected by mining activities. In Portman Bay (SE Spain), both phytotoxkit and ostracodtoxkit has been applied during the risk assessment procedure [38]. The obtained results [8] showed similar results to those obtained in studied samples. The most sensitive bioassay was ostracodtoxkit, and samples strongly affected by mining activities showed a 100% of germination and root inhibition. According to these results, it is highly advisable to apply environmental toxicity testing to characterize the risks presented by contaminated soils.

Other studies in areas affected by phosphate industry wastes [39] suggested that the application of bioassays satisfy the requirements of environmental toxicology in their reliability, sensitivity, reproducibility, rapidity, and low cost. The selected bioassays are an excellent tool in the screening of areas affected by mining exploitation, being correlated with the selected contaminant.

Table 6. Correlation analysis results.

	pH	EC	Pb (mg/kg)	As (mg/kg)	Cd (mg/kg)	Fe (mg/kg)	Zn (mg/kg)	GI *L. Sativum*	GI *S. Alba*	GI *S.Saccharatum*	RI *L. Sativum*	RI *S. alba*	RI *S.Saccharatum*	*PLI*
EC	−0.49 *													
Pb (mg/kg)	−0.25	0.59 *												
As (mg/kg)	−0.40 *	0.59 *	0.40 *											
Cd (mg/kg)	−0.29	0.65 *	0.45 *	0.66 *										
Fe (mg/kg)	−0.48 *	0.53 *	0.31	0.88 *	0.56 *									
Zn (mg/kg)	0.14	0.59 *	0.52 *	0.43 *	0.59 *	0.30								
GI *L. Sativum*	−0.39 *	0.76 *	0.46 *	0.33	0.43 *	0.26	0.51 *							
GI *S. Alba*	−0.61 *	0.70*	0.42 *	0.37*	0.35 *	0.36 *	0.38 *	0.77 *						
GI *S.Saccharatum*	−0.66 *	0.80 *	0.49 *	0.49*	0.50 *	0.48 *	0.36 *	0.70 *	0.86 *					
RI *L. Sativum*	−0.01	0.25	0.14	0.03	0.07	0.01	0.14	0.12	0.14	0.11				
RI *S. alba*	−0.55 *	0.59 *	0.45 *	0.24	0.30	0.28	0.30	0.62 *	0.70 *	0.54 *	0.20			
RI *S.Saccharatum*	−0.64 *	0.65 *	0.52 *	0.29	0.35	0.33	0.20	0.54 *	0.73 *	0.60 *	0.12	0.76 *		
PLI	−0.38 *	0.69 *	0.51 *	0.93 *	0.85 *	0.84 *	0.60 *	0.43 *	0.42 *	0.53 *	0.08	0.35	0.37 *	
NMI	−0.45 *	0.45 *	0.03	0.05	0.03	0.22	−0.14	0.36 *	0.32 *	0.47 *	0.03	0.20	0.29	0.04

* p-value < 0.05; GI: Growht inhibition index (%); RI: Root elongation inhibition index (%).

5. Conclusions

San Quintín mining district was affected by mining activities and surficial soils have undergone weathering processes, releasing a great amount of PTEs, which are transported by torrential rainfalls. The chemical selective extraction could be considered as a powerful tool for the general study of PTE mobility in areas contaminated by mining activities.

Phytotoxkit and Ostracodtoxkit bioassays showed high toxicity of soil samples. The results showed that Class IV (high acute hazard) was represented by 81% of samples and Class V (very high acute hazard) by 15% of samples. Only the reference soil showed Class II (Slight acute hazard). The quality of soils affected by mining activities according to the proposed toxicity classification was better than classification based only in chemical analysis. Moreover, diversified toxic responses indicated a need of microbiotest battery application consisting of acute and chronic tests with the organisms representing different trophic levels.

Author Contributions: Conceptualization: P.H., J.M.E., M.L.G.-L., E.C.-F.; Methodology: E.C.-F., M.L.G.-L., P.H., J.M.E.; Software, E.C.-F., M.L.G.-L., R.S.-D., I.C., P.G.; Investigation, I.C., P.G.; Resources, P.H.; Data Curation, M.L.G.-L., E.C.-F., P.H., J.M.E.; Writing-Original Draft: M.L.G.-L.; Writing-Review & Editing; R.S.-D., M.L.G.-L., E.C.-F., P.H., J.M.E.; Funding Acquisition: P.H.

Funding: This study has been partly funded by Spanish Ministry of Economy and Competitiveness, Project CGL2015-67644-R. Ramón Sánchez-Donoso was supported by the Tatiana Pérez de Guzmán el Bueno Foundation predoctoral scholarship.

Conflicts of Interest: The authors declare no conflict of interest.

References

1. Castillo, S.; de la Rosa, J.; Sánchez de la Campa, J.D.; González-Castanedo, Y.; Fernández-Caliani, J.C.; González, I.; Romero, A. Contribution of mine wastes to atmospheric metal deposition in the surrounding area of an abandoned heavily polluted mining district (Rio Tinto mines, Spain). *Sci. Total Environ.* **2013**, *449*, 363–372. [CrossRef] [PubMed]
2. Valente, T.M.; Leal Gomes, C.L. Occurrence, properties and pollution potential of environmental minerals in acid mine drainage. *Sci. Total Environ.* **2009**, *407*, 1135–1152. [CrossRef] [PubMed]
3. Valente, T.M.; Antunes, M.; Braga, M.A.; Pamplona, J. Geochemistry and mineralogy of ochre-precipitates formed as waste products of passive mine water treatment. *Geochem. Explor. Environ. Anal.* **2011**, *11*, 103–106. [CrossRef]
4. Adamo, P.; Denaix, L.; Terribile, F.; Zampella, M. Characterization of heavy metals in contaminated volcanic soils of the Solofrana river valley (southern Italy). *Geoderma* **2003**, *117*, 347–366. [CrossRef]
5. Muller, G. Index of geoaccumulation in sediments of the Rhine River. *Geojournal* **1969**, *2*, 108–118.
6. Covelli, S.; Fontolan, G. Application of a normalization procedure in determining regional geochemical baselines. *Environ. Geol.* **1997**, *30*, 34–45. [CrossRef]
7. Tomlinson, D.L.; Wilson, J.G.; Harris, C.R.; Jeffrey, D.W. Problems in the assessments of heavy-metal levels in estuaries and formation of a pollution index. *Helgol. Meeresunters.* **1980**, *33*, 566–575. [CrossRef]
8. García-Lorenzo, G.L.; Martínez-Sánchez, M.J.; Pérez-Sirvent, C.; Molina, J. Ecotoxicological evaluation for the screening of areas polluted by mining activities. *Ecotoxicology* **2009**, *18*, 1007–1086. [CrossRef]
9. Rodríguez, L.; Ruiz, E.; Alonso-Azcárate, J.; Rincón, J. Heavy metal distribution and chemical speciation in tailings and soils around a Pb-Zn mine in Spain. *J. Environ. Manag.* **2009**, *90*, 1106–1116. [CrossRef]
10. Martín-Crespo, T.; Gómez-Ortiz, D.; Martín-Velázquez, S.; Esbrí, J.M.; de Ignacio-San José, C.; Sánchez-García, M.J.; Montoya-Montes, I.; Martín-González, F. Abandoned mine tailings in cultural itineraries: Don Quixote Route (Spain). *Eng. Geol.* **2015**, *197*, 82–93. [CrossRef]
11. Higueras, P.; Esbrí, J.M.; García-Ordiales, E.; González-Corrochano, B.; López-Berdonces, M.A.; García-Noguero, E.M.; Alonso-Azcárate, J.; Martínez-Coronado, A. Potentially harmful elements in soils and holm-oak trees (*Quercus ilex* L.) growing in mining sites at the Valle de Alcudia Pb-Zn district (Spain)—Some clues on plant metal uptake. *J. Geochem. Explor.* **2017**, *182*, 166–179. [CrossRef]

12. Sánchez-Donoso, R.; Martín-Duque, J.F.; Crespo, E.; Higueras, P. Tailing's geomorphology of the San Quintín mining site (Spain): Landform catalogue, aeolian erosion and environmental implications. *Environ. Earth Sci.* **2019**, *78*, 166. [CrossRef]
13. Palero-Fernández, F.J.; Martín-Izard, A. Trace element contents in galena and sphalerite from ore deposits of the Alcudia Valley mineral field (Eastern Sierra Morena, Spain). *J. Geochem. Explor.* **2005**, *86*, 1–25. [CrossRef]
14. Rossiter, D. Proposal for a New Reference Group for the World Reference Base for Soil Resources (WRB) 2006: The Technosols. 2005. Available online: http://citeseerx.ist.psu.edu/viewdoc/download;jsessionid=21FBCCD60158CCC50E3D86DCCEA3C5E4?doi=10.1.1.114.1742&rep=rep1&type=pdf (accessed on 5 June 2019).
15. AENOR. *Characterization of Waste. Leaching. Compliance Test for Leaching of Granular Waste Materials and Sludges. Part 4: One Stage Batch Test at a Liquid to Solid Ratio of 10 l/kg for Materials with Particle Size Below 10 mm (without or with Size Reduction)*; AENOR: Madrid, Spain, 2003.
16. Chung, F.H. Quantitative interpretation of X-ray diffraction patterns. I. Matrix-flushing method of quantitative multicomponent analysis. *J. Appl. Crystallogr.* **1974**, *7*, 519–525. [CrossRef]
17. Chung, F.H. Quantitative interpretation of X-ray diffraction patterns. III. Simultaneous determination of a set of reference intensities. *J. Appl. Crystallogr.* **1975**, *8*, 17–19. [CrossRef]
18. Jorfi, S.; Maleki, R.; Jaafarzadeh, N.; Ahmadi, M. Pollution load index for heavy metals in Mian-Ab plain soil, Khuzestan, Iran. *Data Brief.* **2017**, *15*, 584–590. [CrossRef] [PubMed]
19. García-Lorenzo, M.L.; Pérez-Sirvent, C.; Molina-Ruiz, J.; Martínez-Sánchez, M.J. Mobility indices for the assessment of metal contamination in soils affected by old mining activities. *J. Geochem. Explor.* **2014**, *147*, 117–129. [CrossRef]
20. OECD. *Guideline of the OECD for Testing Chemical Products-Terrestrial Plants*; Growth Test Method, 208; OECD: Paris, France, 1984.
21. Phytotoxkit. Seed Germination and Early Growth Microbiotest with Higher Plants. In *Standard Operation Procedure*; MicroBioTests Inc.: Gent, Belgium, 2004; pp. 1–34.
22. Liu, J.; Dazzo, F.B.; Glagoleva, O.; Yu, B.; Jain, A.K. CMEIAS: A computer-aided system for the image analysis of bacterial morphotypes in microbial communities. *Microb. Ecol.* **2001**, *41*, 173–194. [CrossRef] [PubMed]
23. Ostracodtoxkit, F. "Direct Contact" Toxicity Tests for Freshwater Sediments. In *Standard Operational Procedure*; MicroBioTests Inc.: Gent, Belgium, 2001; pp. 1–37.
24. Persoone, G.; Marsalek, B.; Blinova, I.; Torokne, A.; Zarina, D.; Manusadzianas, L.; Nalecz-Jawecki, G.; Tofan, L.; Stepanova, N.; Tothova, L.; et al. A practical and user-friendly toxicity classification system with microbiotests for natural waters and wastewaters. *Environ. Toxicol.* **2003**, *18*, 395–402. [CrossRef] [PubMed]
25. Clark, I. Practical Geostatistics. Geostokos Ltd., Central Scotland. 2001, p. 19. Available online: http://www.kriging.com/PG1979/PG1979.pdf (accessed on 15 April 2019).
26. Jiménez Ballesta, R.; Conde Bueno, P.; Martín Rubí, J.A.; García Giménez, R. Niveles de fondo geoquímico e influencia del marco geológico en las concentraciones edafoquímicas de base de suelos seleccionados de Castilla-La Mancha. *Estudios Geológicos* **2010**, *66*, 123–130. [CrossRef]
27. Bravo, S.; García-Ordiales, E.; García-Navarro, F.J.; Amorós, J.A.; Pérez-de-los-Reyes, C.; Jiménez-Ballesta, R.; Esbrí, J.M.; García-Noguero, E.M.; Higueras, P. Geochemical distribution of major and trace elements in agricultural soils of Castilla-La Mancha (central Spain): Finding criteria for baselines and delimiting regional anomalies. *Environ. Sci. Pollut. Res.* **2019**, *26*, 3100–3114. [CrossRef] [PubMed]
28. Navarro, M.C.; Pérez-Sirvent, C.; Martínez-Sánchez, M.J.; Vidal, J.; Tovar, P.J.; Bech, J. Abandoned mine sites as a source of contamination by heavy metals: A case study in a semi-arid zone. *J. Geochem. Explor.* **2008**, *96*, 183–193. [CrossRef]
29. Oyarzun, R.; Lillo, J.; López García, J.A.; Esbrí, J.M.; Cubas, P.; Llanos, W.; Higueras, P. The Mazarrón Pb-(Ag)-Zn mining district (SE Spain) as a source of heavy metal contamination in a semiarid realm: Geochemical data from mine wastes, soils, and stream sediments. *J. Geochem. Explor.* **2011**, *109*, 113–124. [CrossRef]
30. Schwartz, M.O. Cadmium in zinc deposits: Economic geology of a polluting element. *Int. Geol. Rev.* **2000**, *42*, 445–469. [CrossRef]
31. Lin, Y.; Tiegeng, L. Sphalerite chemistry, Niujiaotang Cd-rich zinc deposit, Guizhou, Southwest China. *Chin. J. Geochem.* **1999**, *18*, 62–68. [CrossRef]
32. O'Day, P.A. Chemistry and mineralogy of arsenic. *Elements* **2006**, *2*, 77–83. [CrossRef]

33. Seaman, J.C.; Bertsch, P.M.; Strom, R.N. Characterization of colloids mobilized from southeastern coastal plains sediments. *Environ. Sci. Technol.* **1997**, *31*, 2782–2790. [CrossRef]
34. Smith, K.S. Metal Sorption on Mineral Surfaces: An Overview with Examples Relating to Mineral Deposits. In *The Environmental Geochemistry of Mineral Deposits*; Reviews in Economic Geology; Plumlee, G.S., Logsdon, M.J., Eds.; Society of Economic Geologists: Chelsea, MI, USA, 1999; pp. 161–182.
35. Smedley, P.L.; Kinniburgh, D.G. A review of the source, behaviour and distribution of arsenic in natural waters. *Appl. Geochem.* **2002**, *17*, 517–568. [CrossRef]
36. Meng, X.; Korfiatis, G.P.; Bang, S.; Bang, K.W. Combined effects of anions on arsenic removal by iron hydroxides. *Toxicol. Lett.* **2002**, *133*, 103–111. [CrossRef]
37. Kohler, U.; Luniak, M. Data inspection using biplots. *Stata J.* **2005**, *5*, 208–223. [CrossRef]
38. Martínez-Sánchez, M.J.; Pérez-Sirvent, C.; García-Lorenzo, M.L.; Martínez-López, S.; Bech, J.; Hernández, C.; Martínez, L.B.; Molina, J. Ecoefficient In Situ Technologies for the Remediation of Sites Affected by Old Mining Activities: The Case of Portman Bay. In *Assessment, Restoration and Reclamation of Mining Influenced Soils*; Bech, J., Bini, C., Pashkevich, M.A., Eds.; Academic Press: Cambridge, MA, USA, 2017; pp. 355–373. [CrossRef]
39. Martínez-Sánchez, M.J.; Pérez-Sirvent, C.; García-Lorenzo, M.L.; Martínez-López, S.; Bech, J.; García-Tenorio, R.; Bolívar, J.P. Use of bioassays for the assessment of areas affected by phosphate industry wastes. *J. Geochem. Explor.* **2014**, *147*, 130–138. [CrossRef]